Evidence of Carotenoid in Surgically Removed Lamellar Hole-Associated Epiretinal Proliferation

Akira Obana,[1,2] Hiroyuki Sasano,[1] Shigetoshi Okazaki,[2] Yoshiro Otsuki,[3] Takahiko Seto,[1] and Yuko Gohto[1]

[1]Department of Ophthalmology, Seirei Hamamatsu General Hospital, Naka-ku, Hamamatsu City, Shizuoka, Japan
[2]Department of Medical Spectroscopy, Institute for Medical Photonics Research, Preeminent Medical Photonics Education & Research Center, Hamamatsu University School of Medicine, Hamamatsu, Shizuoka, Japan
[3]Department of Pathology, Seirei Hamamatsu General Hospital, Naka-ku, Hamamatsu City, Shizuoka, Japan

Correspondence: Akira Obana, Department of Ophthalmology, Seirei Hamamatsu General Hospital, 2-12-12 Sumiyoshi, Naka-ku, Hamamatsu City, Shizuoka, 430-8558, Japan; obana@sis.seirei.or.jp.

Submitted: June 2, 2017
Accepted: September 12, 2017

Citation: Obana A, Sasano H, Okazaki S, Otsuki Y, Seto T, Gohto Y. Evidence of carotenoid in surgically removed lamellar hole-associated epiretinal proliferation. *Invest Ophthalmol Vis Sci*. 2017;58:5157–5163. DOI: 10.1167/iovs.17-22347

Purpose. To determine the constituents and origin of the yellow pigment in surgically removed lamellar hole-associated epiretinal proliferation (LHEP) in patients with lamellar macular hole (LMH).

Methods. This prospective case series comprised nine eyes with LMH in patients aged 41 to 83 years. The presence of LHEP was confirmed by preoperative optical coherence tomography; the distribution of macular pigment was observed by two-wavelength fundus autofluorescence technique before and after surgery. The subjects underwent a 25-gauge vitrectomy, and the surgically removed epiretinal membranous tissue was fixed with formalin. The specimens were examined using resonance Raman microscopy, and paraffin sections were stained with antiglial fibrillary acidic protein.

Results. Seven cases presented with LHEP, and the presence of yellow pigment was confirmed using an operating microscope. Carotenoid-specific Raman signals with three major Raman peaks could be identified in the specimens with LHEP. These specimens were positive for glial fibrillary acidic protein staining. Using the fundus autofluorescence technique, a central defect in the distribution of the macular pigment was noted in the exact area of the lamellar hole. This type of defect was no longer visible after surgical repair of the lamellar hole.

Conclusions. The constituents of the yellow pigment in the removed LHEP were carotenoids that typically originate from the macular xanthophyll pigments at the fovea. Since LHEP is reported to be composed of Müller cells, we hypothesize that xanthophyll carotenoids at the fovea are contained in the Müller cells.

Keywords: lamellar macular hole, lamellar hole-associated epiretinal proliferation, xanthophyll carotenoids, Müller cell cone, resonance Raman microscopy

Lamellar macular hole (LMH) was first described by Gass in 1976.[1] He made a clinicopathological case report on aphakic cystoid macular edema and suggested that LMH in that case was caused by a rupture of the inner wall in cystoid macular edema. With the progress of optical coherence tomography (OCT), the pathophysiological details of LMH have been revealed by many investigators, and it is now considered a disorder related to abnormalities of the vitreoretinal interface. However, the definition of LMH and a clear distinction from other disorders with vitreoretinal interface syndrome, such as macular pseudohole (MPH), have not been fully established, and the mechanisms of LMH development have not been fully elucidated. OCT findings show that LMH is associated with the epiretinal membrane (ERM). Witkin et al.[2] found a thick ERM at the margin of an inner defect of LMH that had different characteristics from typical contractile ERM. The same membrane was reported as a "dense non-tractional ERM"[3] and "atypical epiretinal tissue."[4] Pang et al.[5] referred to these thick or dense ERMs as lamellar hole-associated epiretinal proliferation (LHEP). They suggested that LHEP is a distinct clinical entity and LMH with LHEP has a poorer visual acuity, larger hole diameter, thinner retina, and higher incidence of ellipsoid disruption than LMH without LHEP.[6] These findings were supported by other investigations.[7] The baseline visual acuity, as well as improvement of visual acuity after surgery, has been reported as worse in LMH with LHEP,[8] although the results are controversial.[7] Govetto et al.[9] suggested the possibility of three different mechanisms underlying the development of LMH, degenerative LMH, tractional LMH, and a combination of them. They suggested that LHEP was associated with degenerative LMH; thus, LHEP is a very important characteristic sign to consider the mechanism of LMH development and its prognosis. However, the origin of LHEP has not been determined. Pang et al.[10] argued that LHEP originates from the Müller cells in association with retinal defects, and revealed that LHEP was histopathologically composed of proliferated Müller cells. On the contrary, Compera et al.[11] mentioned that LHEP originated from the vitreous and comprised fibroblasts, hyalocytes, and type II collagen.

LHEP typically appears yellowish[10] when it is removed surgically. Since no yellow pigment is reported to exist in the retina other than macular pigment, the yellow pigment in LHEP is speculated to be related to the carotenoids of macular pigment. However, it has not been proven that the yellow

pigment is composed of xanthophyll carotenoid of the macular pigment. If LHEP contains macular pigment, the possibility that LHEP originates from the retina becomes high. In this study, we investigated the constituents of the yellow pigment in LHEP by resonance Raman microscopy (RRM).

The macular pigment consists of three xanthophyll carotenoids, lutein ([3R,3′R,6′R]-lutein), zeaxanthin ([3R,3′R]-zeaxanthin), and *meso*-zeaxanthin ([3R,3′S;*meso*]-zeaxanthin).[12,13] It is mainly present in the outer plexiform layer (also called the Henle fiber layer), which is composed of the axons of the cone photoreceptors; it is also present in the inner plexiform layer.[13,14] Xanthophyll carotenoid is thought to be contained in the retina, bound to carotenoid-specific receptor proteins, namely, glutathione S-transferase P1 (GSTP1) for zeaxanthin[15] and steroidogenic acute regulatory domain protein 3 (StARD3) for lutein.[16] However, it is still unknown whether these receptor proteins exist in the cell membranes of neural axons or glial cells in the outer and inner plexiform layers. The current results provide some indication for the exact cells that contain xanthophyll pigments.

Subjects and Methods

Subjects and Assessment of Preoperative OCT Findings

Nine eyes of nine subjects with LMH underwent vitrectomy from March 2016 to April 2017 in the Department of Ophthalmology, Seirei Hamamatsu General Hospital. Patients were 41 to 83 years old (mean = 70.3, SD = 13.3 years old), comprising five men and four women.

Preoperative OCT (Cirrus OCT, Carl Zeiss Meditec, Inc., Tokyo, Japan; Spectralis OCT, Heidelberg Engineering, Heidelberg, Germany) images of each case were evaluated. According to previous reports,[2,4,5] ERMs are divided into two types: (1) "typical ERM," which are relatively thin and hyperreflective membranes with contractile properties; and (2) "LHEP," which are thick or dense ERMs with homogeneous medium reflectivity and no contractile properties.

Observation of the Distribution of Macular Pigment

The distribution of macular pigment was observed by the two-wavelength fundus autofluorescence technique before and after surgery. The prototype macular pigment optical density (MPOD) module on Heidelberg Spectralis with MultiColor (Spectralis-MP, Heidelberg Engineering) was used. This devise used two wavelengths light (486 nm, 518 nm). The basic mechanism and handling of this instrument is described elsewhere.[17,18] The pupil was dilated to at least 7 mm diameter using a topical mydriatic agent. After taking autofluorescent images, a macular pigment optical density map was constructed with the prototype software. The reference point was set to 9° eccentricity. Spectralis OCT B-scan images were imposed on the distribution pictures, and the exact layers that the macular pigment existed in the retina were evaluated.

Surgical Procedure and Observation of Yellow Pigments Under the Operating Microscope

All subjects underwent a 25-gauge vitrectomy. After removing the vitreous gel and the posterior hyaloid, following creation of a triamcinolone-assisted posterior vitreous detachment, the ERM was removed along with the internal limiting membrane (ILM) using microforceps. If the ERM was removed without the ILM, the latter was subsequently peeled using the triamcinolone-

Table. Patients Characteristics and Summary of the Results

Subject	Age, y	Sex	Preoperative Visual Acuity, logMAR	Postoperative Visual Acuity, logMAR	OCT Findings		Yellow Pigment in the Removed Membrane	Raman Signal	Preoperative Macular Pigment Distribution	Postoperative Macular Pigment Distribution	GFAP Staining
					LHEP	Typical ERM					
1	83	Female	0.52	0.22	y	y	Positive	Positive	-	-	Positive
2	68	Male	0.30	0.40	y	y	Positive	Positive	-	-	Positive
3	59	Female	0.22	0.15	y	n	Positive	-	-	-	-
4	41	Female	0.05	0	y	y	Positive	Positive	-	-	Positive
5	74	Female	0.40	0	n	n	Negative	Negative	CD	Disk	-
6	73	Male	0.52	0	y	y	Positive	-	CD	CD	-
7	79	Male	0.40	0.05	n	y	Negative	-	CD	Disk	-
8	73	Male	0.30	0	y	y	Positive	Positive	Impossible	Disk	-
9	83	Male	0.52	0.70	y	n	Positive	Positive	Impossible	Disk	-

En dash indicates examination was not performed. CD, central defect of macular pigment; Disk, no central defect and disk-shaped distribution; n, no; y, yes.

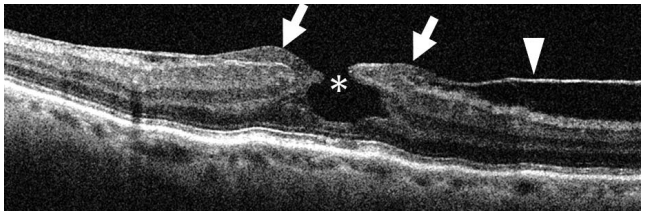

FIGURE 1. OCT image (*vertical line scan*) of the eye showing a LMH (Subject No. 1 in the Table). *Arrows* show a LHEP. Typical ERM continuous with the LHEP (*arrowhead*) extends toward the periphery and is separated from the surface of the retina at upper side of the lamellar hole. Splitting of Henle's layer and a break in the inner retinal layers (*) is noted.

assisted technique. No staining agents such as brilliant blue or indocyanine green were used. Phacoemulsification with intraocular lens implantation was performed on all patients.

The ERM was carefully observed for the presence of yellow pigment while peeling it from the retinal surface. The removed tissue was immediately placed on a glass slide, and the presence of yellow pigment was determined under the operating microscope (OPMI Lumera 700, Carl Zeiss Meditec, Inc.) by the surgeon and an assistant doctor. The results were later confirmed using DVD video recordings. The removed ERM was immediately fixed using a 20% formalin fixative.

The operation was carried out by one surgeon (OA) as part of the routine clinical practice after obtaining informed consent, but the use of the removed tissue for the purpose of research was approved by the institutional review board of Seirei Hamamatsu General Hospital (No. 2042). Patients signed an informed consent form, which stated that the study complied with the tenets of the Declaration of Helsinki.

Observation With RRM

RRM can identify a carotenoid based on its characteristic Raman scattering response. Lutein, meso-zeaxanthin, and zeaxanthin, when excited by resonant wavelength light, show three major Raman peaks at 1008, 1159, and 1525 cm^{-1}, which correspond to the rocking motions of the methyl components ($C\text{-}CH_3$), and the stretch vibrations of the carbon-carbon single bonds (C-C) and double bonds (C=C).[19] These characteristic Raman signals revealed the existence of carotenoids in the specimen. The sample tissue fixed using formalin fixative was placed on a glass slide and excised by a diode laser of 488 nm wavelength (85 BCD 010, CVI Melles Griot, Carlsbad, CA, USA) installed on the microscope (IX81, Olympus, Tokyo, Japan). The diameter of illumination spot was 6 μm. The Raman signals were detected by a photonic multichannel analyzer (PMA-50, Hamamatsu Photonics, Shizuoka, Japan).

Histological Observation

Sample tissues were embedded in paraffin using routine techniques. Section specimens of 3-μm thickness were stained using hematoxylin and eosin and observed under light microscopy (BX53, Olympus, Tokyo, Japan). For immunohistochemical observation, the section specimens were stained with antiglial fibrillary acidic protein (anti-GFAP) antibodies (clone 6F2, dilution 1:200, DAKO, Glostrup, Denmark).

Results

Patient characteristics, pre- and postoperative visual acuity, and a summary of the results are shown in the Table. Visual acuity measured using a decimal visual acuity test chart was converted to logMAR. Postoperative visual acuity was the value 1 month after the surgery. Five eyes showed a >0.3 logMAR improvement in visual acuity after surgery, and the other four eyes had no change in visual acuity within 0.3 logMAR. No complications occurred during the surgical procedures.

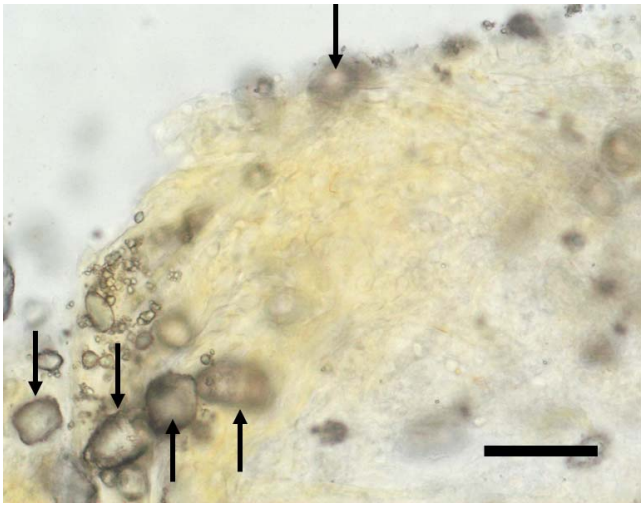

FIGURE 2. Light microscopy of the specimen from Subject No. 2 in the Table. The removed membrane looks yellowish. Triamcinolone particles (*arrows*) are present (no stain; *scale bar*: 100 μm).

Seven eyes showed LHEP in the preoperative OCT images (Fig. 1). In these eyes, the yellow pigment appeared to extend from the margin of the lamellar hole to the surrounding thick ERM that corresponded to LHEP intraoperatively; yellow pigments were noted in the surgically removed thick membrane under the operating microscope and light microscope (Fig. 2). ILM was peeled separately with the thick membrane in five of these seven eyes, and no pigment was noted in the ILM. Two eyes that had no LHEP before surgery did not show yellow pigment in the removed membrane.

Resonance Raman microscopic observation was performed in six eyes. Other three eyes were not examined owing to the following reasons: one tissue was lost when it was extracted from the eye, one was insufficient for a specimen, and the yellow-tinged portion of one was lost when the flat specimen

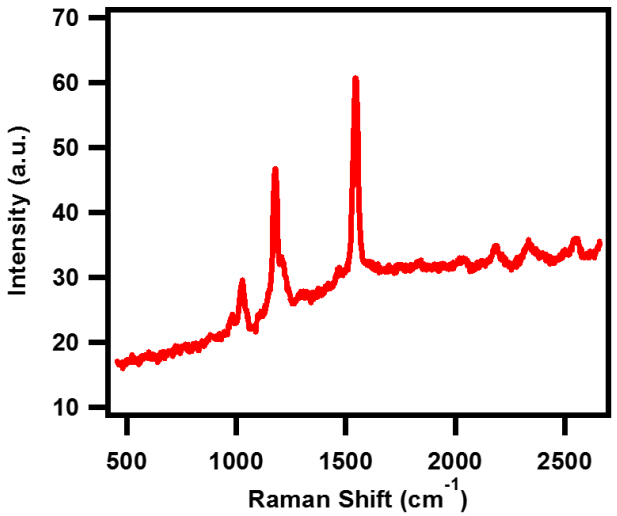

FIGURE 3. Raman signals of the specimen from Subject No. 1 in the Table. Three carotenoid-specific peaks are noted.

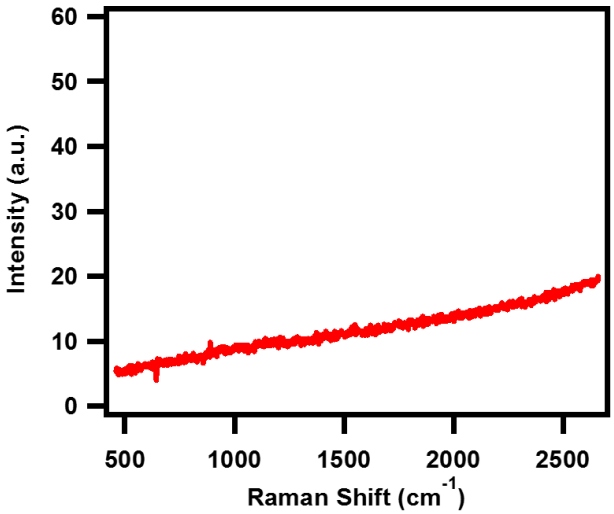

FIGURE 4. Raman signals of the specimen from Subject No. 5 in the Table. No carotenoid-specific peaks are noted.

was made. Carotenoid-specific Raman signals (Fig. 3) were identified in five specimens that showed LHEP in the preoperative OCT images and yellow pigment under operation microscopy (Table). No carotenoid-specific Raman signals were found in one eye that had no LHEP (Fig. 4), and there was no yellow pigment in the removed membrane.

The distribution images of the macular pigment were acquired for five eyes. Pre- and postoperative images were acquired for three eyes, and only postoperative images were acquired for two eyes. The preoperative images of these two eyes could not be obtained due to cataracts. Prior to surgery, the central defect of macular pigment at the area corresponding to the lamellar hole was observed in all three eyes examined, and the lamellar hole was surrounded by macular pigment (Fig. 5A). In two of these three eyes, the central defect of macular pigment resolved with repair of the central depression of the lamellar hole after surgery (Fig. 5B). Disc-shaped macular pigment was observed after surgery in four of five eyes. Figure 5B shows an interesting finding. A small defect was noted in the disc-shaped macular pigment, and this defect corresponded to a small cyst in the Henle fiber layer depicted on the OCT B-scan image. This result suggested that macular pigment at the surrounding area of the fovea existed in the Henle fiber layer. In one case that had LHEP prior to surgery, the irregularly shaped pigmentation was observed surrounding the hole, and this pigmented area corresponded to the extent of LHEP observed in the OCT B-scan image (Fig. 6A). This irregularly shaped pigment was no longer observed with the removal of LHEP (Fig. 6B). In this eye, a lamellar hole was repaired 1 month after the initial surgery, but depression at the fovea was steeper than the normal foveal curvature. Therefore, the central defect of macular pigment was still present, and the macular pigment surrounding central defect was noted instead of pigments with LHEP.

The specimens from three eyes were examined histologically. Light microscopy with hematoxylin and eosin stain showed extracellular matrix with cell component, and immunohistochemical staining with anti-GFAP was positive (Fig. 7).

DISCUSSION

In all eyes that showed LHEP by OCT, the presence of yellow pigment was confirmed in the removed tissue by examination under the operating microscope and light microscope. Five were examined with RRM, and carotenoid-specific Raman signals were confirmed in all specimens examined. The one eye that did not have LHEP by OCT showed no specific Raman signals. These results proved that yellow pigments in LHEP were composed of carotenoid pigments. Since human maculae contain carotenoids composed of lutein, zeaxanthin, and meso-zeaxanthin,[12,13] the yellow pigments in LHEP were considered to originate from macular xanthophyll carotenoids.

Pang et al.[10] demonstrated histologically that LHEP was composed of proliferated Müller cells and argued that LHEP originates from the retina.[5] The GFAP-positive immunostaining of LHEP in the present study corroborated their findings. The findings that LHEP was composed of Müller cells and contained macular pigment indicates the possibility that Müller cells contain xanthophyll carotenoids. The possibility that Müller cells have carotenoids has been mentioned by Gass in 1999.[20] He presented the cone-shaped zone of Müller cells at the fovea (anatomically; foveola) as Müller cell cone and hypothesized

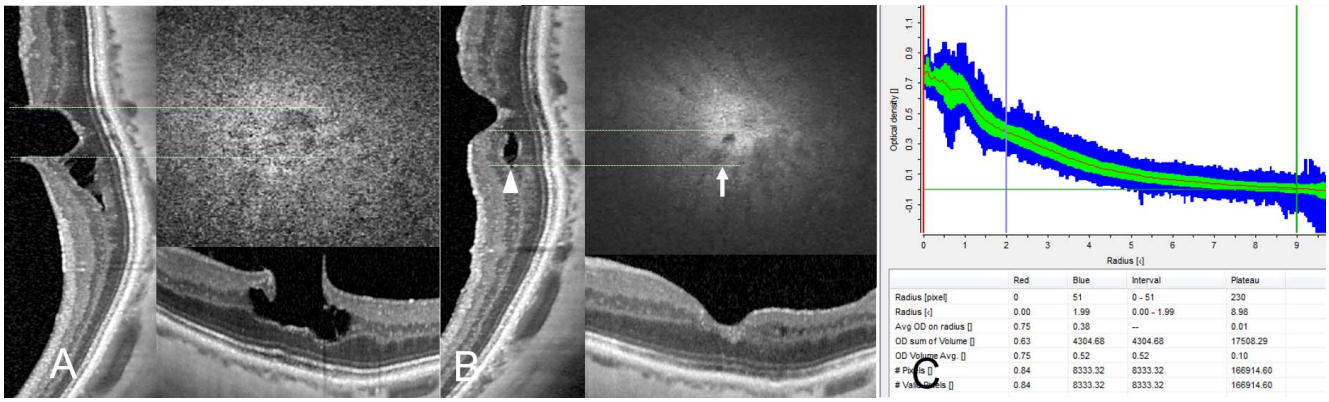

FIGURE 5. Macular pigment distribution images and OCT images of vertical and horizontal line scan (Subject No. 7 in the Table). The transverse size of the OCT images was adjusted to the macular pigment distribution image. (**A**) Before surgery, a central defect of macular pigment corresponded to the lamellar hole (between the two *dotted lines*). Macular pigment expanded at the surrounding area of lamellar hole. The low contrast of macular pigment was due to cataract. (**B**) One month after surgery, there was no central defect and a disc-shaped macular pigment was noted. A small defect in the disc-shaped macular pigment (*arrow*) corresponded to a small cyst in the Henle fiber layer (*arrowhead*) represented by the *vertical line* scan OCT image (between the two *dotted lines*). (**C**) Mean macular pigment density profile with standard deviations (*green bars*) and maximum and minimum values (*blue bars*) 1 month after surgery. The value is a mean of the optical density at the given radius around the center. There was no central defect and the optical density at the center (*red line*) was 0.75. The *green line* represents the reference point at 9° eccentricity.

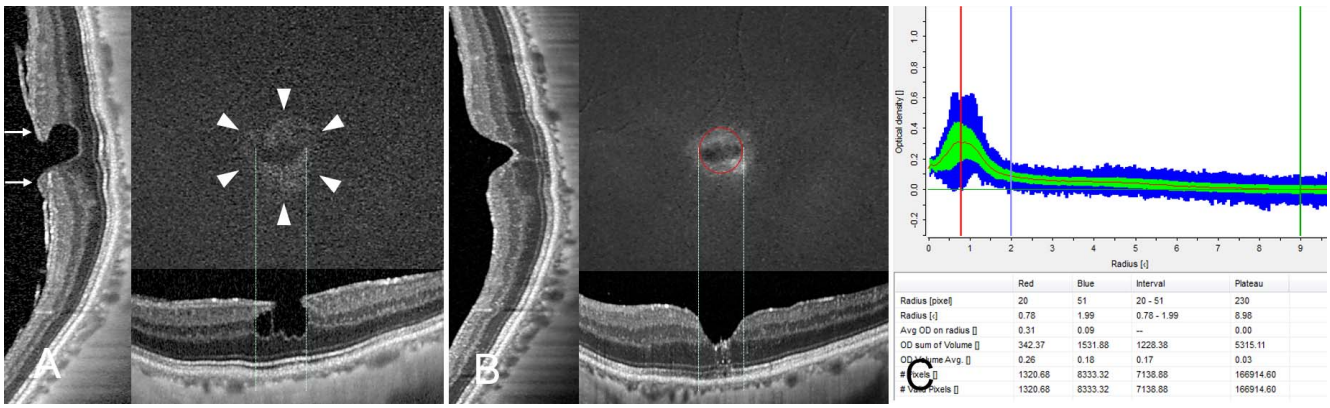

Figure 6. Macular pigment distribution images and OCT images of the *vertical* and *horizontal line scan* (Subject No. 6 in the Table). The transverse size of the OCT images was adjusted to macular pigment distribution image. (**A**) Before surgery, a central defect of the macular pigment corresponded to the lamellar hole (between the two *dotted lines*). An irregularly shaped macular pigmentation was observed surrounding the hole (*arrowheads*), and this pigmented area corresponded to the extent of LHEP observed in the OCT images (*arrows*). The low contrast of macular pigment was due to cataract. (**B**) One month after surgery, the lamellar hole was repaired but the depression at the fovea was a little steeper than the normal foveal curvature, and a central defect of macular pigment was noted (between the two *solid lines*). The shape and size of macular pigment expanded around the lamellar hole was different from the irregularly shaped pigmentation in Fig. 6A. The size of the pigment area was smaller than the irregularly shaped pigmentation. The *red circle* represents 0.78° eccentricity that corresponded to the *red line* in Figure 5C. (**C**) Mean macular pigment density profile with standard deviations (*green bars*) and maximum and minimum values (*blue bars*). An optical density defect was noted at the center and the highest density was 0.31 at 0.78° eccentricity (*red line*). The *green line* represents a reference point at 9° eccentricity.

that the Müller cell cone is a reservoir for macular carotenoid pigments. The present results support this hypothesis.

The mechanisms of lamellar hole development have not been proved, but the present results suggest the importance of Müller cells at the fovea. Gass[20] hypothesized that the Müller cells at the fovea (Müller cell cone) serve as a plug to bind together the photoreceptor cells in the foveola, and the degeneration of the Müller cell cone plays an important role to develop a full-thickness macular hole. In the LMH, a similar mechanism may be applicable. In the present study, macular pigment was absent from the site of the LMH as shown by macular pigment distribution images. This result suggests a lack of Müller cells at the bottom of the lamellar hole. Additionally, when the hole was surgically repaired and the central depression resolved, macular pigment appeared at the fovea. This result suggests that the lamellar hole was repaired by the proliferative Müller cells that contain xanthophyll carotenoids. The same findings were obtained in our full thickness macular hole cases (Sasano H, unpublished data, 2017). In the case where the central defect of macular pigment remained after surgery (Figs. 6B, 6C), the Müller cells may not have sufficiently proliferated.

In the images showing the distribution macular pigment, pigment expanded in the area surrounding the fovea. As shown in Figure 5B, the macular pigment in this area existed in the Henle fiber layer at the parafovea. Therefore, we

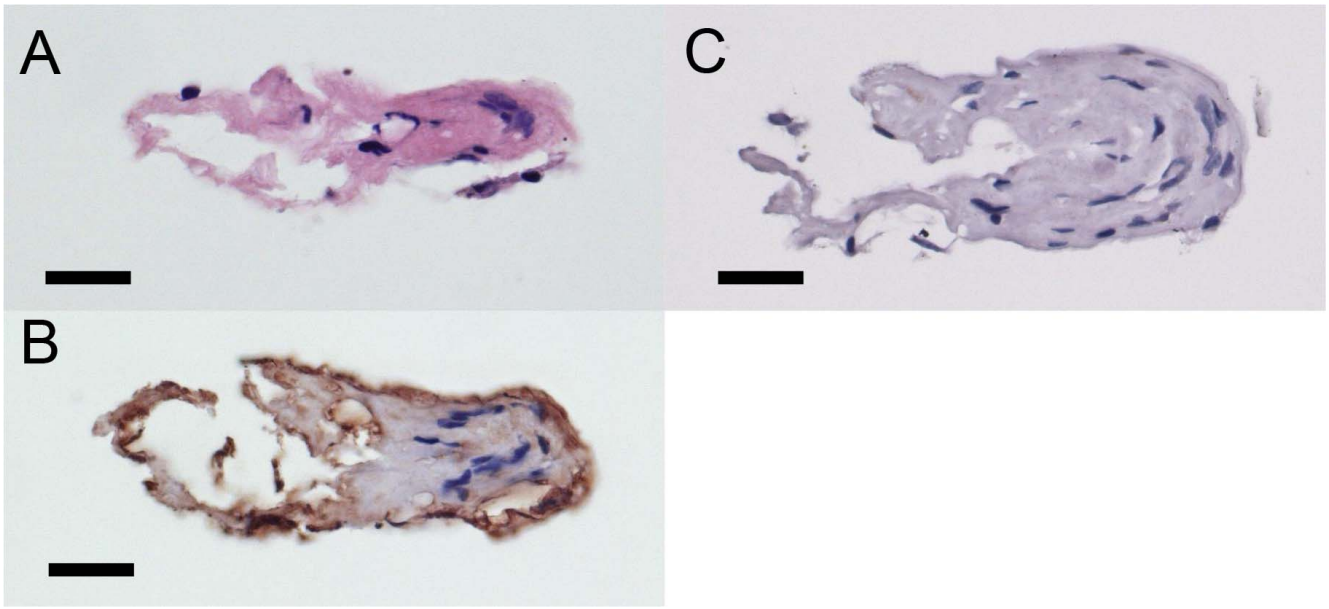

Figure 7. Histology and immunocytochemistry of the removed ERM of the eye with a LMH (Subject No. 2 in the Table). (**A**) Light microscopy with hematoxylin and eosin stain showing extracellular matrix with cell component (*scale bar*: 25 μm). (**B**) Light microscopy with anti-GFAP stain showing positive staining (*scale bar*: 25 μm). (**C**) Light microscopy of the negative control of anti-GFAP stain (*scale bar*: 25 μm).

Investigative Ophthalmology & Visual Science

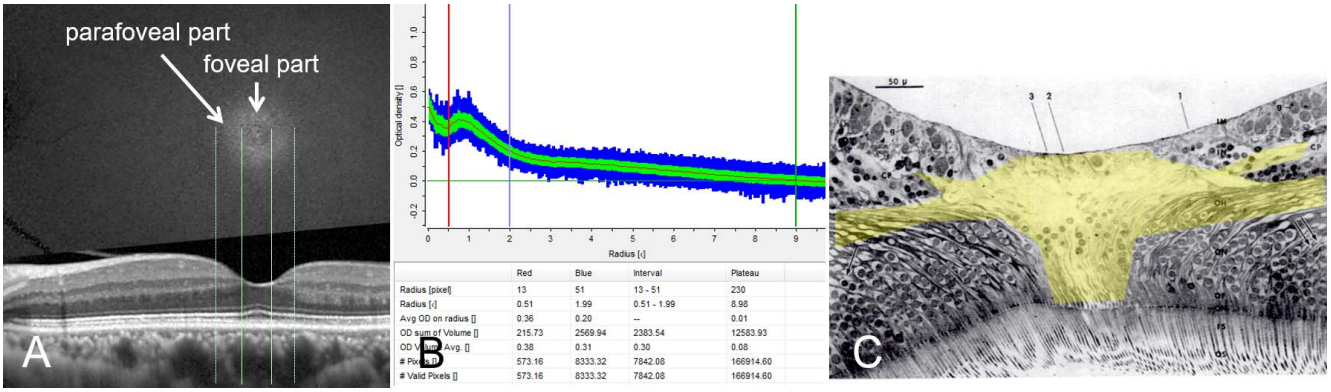

Figure 8. (**A**) Macular pigment distribution images and OCT images of the *vertical line* scan of the eye without macular disorders. The transverse size of OCT images was adjusted to the macular pigment distribution image. Macular pigment is considered to be composed of two portions. The central portion corresponds to the fovea (between the two *solid lines*) and a ring-like portion surrounding the central portion corresponds to the parafovea (between two *dotted lines*). The *solid lines* corresponded to the *red line* at 0.51° eccentricity, and the *dotted lines* corresponded to the *blue line* at 1.99° eccentricity in Figure 8B, respectively. (**B**) The mean macular pigment density profile with standard deviations (*green bars*) and maximum and minimum values (*blue bars*). The central side from the *red line* (the radius; 0.51°) corresponded to the fovea. The area between the *red* and *blue lines* corresponded to the parafovea. (**C**) Schematic image of the existence of macular pigment. At the fovea (foveola), pigment is present in the Müller cell cone and expands into the Henle fiber layer and inner plexiform layer at the parafovea. Modified from Yamada E. Some structural features of the fovea centralis in the human retina. *Arch Ophthalmol.* 1969;82:151–159. Reprinted with permission. © 1969 American Medical Association. All rights reserved.[21]

hypothesized that macular pigment is composed of two parts (Fig. 8). Macular pigment at the fovea (foveola) exists in the Müller cells (Müller cell cone) and macular pigment at the parafovea exists mainly in Henle fiber layer. However, the exact cells that contain pigment in the Henle fiber layer are unknown and could be the Müller cells or axon fibers of the cone.

The present study has some limitations. Our histological analysis was preliminary, and we cannot definitively conclude that LHEP originates either from the retina[5,10] or from the vitreous.[3,4] Our present RRM results also cannot show that carotenoid-specific signals come from the Müller cells. RRM observation was carried out in specimens prior to the preparation of the paraffin specimens. It was impossible to measure Raman signals on the immunostained paraffin sections because xanthophyll carotenoids dissolve in alcohol during dehydration. Therefore, it could not be determined where the lesion measured by RRM coincided with the GFAP-positive lesion. The possibility that xanthophyll originates from other cells is undeniable. We are planning to examine immunohistochemical double staining using antibodies to the receptor proteins of xanthophyll carotenoids, StARD3 and GSTP1, and GFAP to overcome this obstacle. Spectralis-MP was not available when we began this study; thus, the small number of eyes from which the macular pigment distribution images were taken is another limitation. We have obtained similar findings in our study on full thickness macular hole cases (Sasano H, unpublished data, 2017), but the location of the macular pigment in the parafovea should be studied in a larger case series. We cannot obtain clear images of macular pigment in eyes with cataract using Spectralis-MP. Relatively low contrast images, such as those in Figures 5A and 6A, were due to the influence of cataract. MPOD cannot be compared directly between eyes with cataract and eyes with implanted intraocular lenses because the rate of laser light transmission is different; however, the distribution pattern identified with Spectralis-MP is not affected even if the eyes have nuclear cataract, because nuclear cataract uniformly obscures laser light transmission. The present five cases had nuclear cataract and no irregular opacity of the lens. Therefore, the results in the distribution of macular pigment before surgery were considered acceptable.

The constituents of the yellow pigment in the removed LHEP were carotenoids that supposedly originated from macular xanthophyll pigments at the fovea. Since LHEP is reported to be composed of Müller cells, we concluded that xanthophyll carotenoids at the fovea were contained in the Müller cells, although more direct proof is needed. The lack of macular pigments corresponding to the lamellar hole suggests a defect of Müller cells at the bottom of the lamellar hole, and this central defect resolved with the surgical repair of the lamellar hole. Müller cells at the fovea (Müller cell cone) containing xanthophyll carotenoids were supposed to play an important role in the development of LMH. Macular pigment surrounding the lamellar hole at the parafovea was considered to exist in the Henle fiber layer. The exact cells that contain xanthophyll carotenoids in this layer are unknown and require further investigation.

Acknowledgments

The authors thank Editage (www.editage.jp) for English language editing.

This study was presented at the ARVO annual meeting, Baltimore, Maryland, United States, May 2017, as a poster (5021).

Disclosure: **A. Obana**, None; **H. Sasano**, None; **S. Okazaki**, None; **Y. Otsuki**, None; **T. Seto**, None; **Y. Gohto**, None

References

1. Gass JDM. Lamellar macular hole: a complication of cystoid macular edema after cataract extraction. *Arch Ophthalmol.* 1976;94:732–739.
2. Witkin AJ, Ko TH, Fujimoto JG, et al. Redefining lamellar hole and the vitreomacular interface: an ultrahigh-resolution optical coherence tomography. *Ophthalmology.* 2006;113:388–397.
3. Parolini B, Schumann RG, Cereda MG, et al. Lamellar macular hole: a clinicopathologic correlation of surgically excised epiretinal membranes. *Invest Ophthalmol Vis Sci.* 2011;52:9074–9083.
4. Schumann RG, Compera D, Schaumberger MM, et al. Epiretinal membrane characteristics correlate with photore-

ceptor layer defects in lamellar macular holes and macular pseudoholes. *Retina*. 2015;35:727–735.

5. Pang CE, Spaide RF, Freund KB. Epiretinal proliferation seen in association with lamellar macular holes. A distinct clinical entity. *Retina*. 2014;34:1513–1523.
6. Pang CE, Spaide R, Freund KB. Comparing functional and morphological characteristics of lamellar macular holes with and without lamellar hole-associated epiretinal proliferation. *Retina*. 2015;35:720–726.
7. Dell'omo R, Virgili G, Rizzo S, et al. Role of lamellar hole-associated epiretinal proliferation in lamellar macular holes. *Am J Ophthalmol*. 2017;175:16–29.
8. Ko J, Kim GA, Lee SC, et al. Surgical outcomes of lamellar macular holes with and without lamellar hole-associated epiretinal proliferation. *Acta Ophthalmol*. 2016;95:e221–e226.
9. Govetto A, Dacquay Y, Farajzadeh M, et al. Lamellar macular hole: two distinct clinical entities? *Am J Ophthalmol*. 2016;164:99–109.
10. Pang CE, Maberley DA, Freund KB, et al. Lamellar hole-associated epiretinal proliferation. A clinicopathologic correlation. *Retina*. 2016;36:1408–1412.
11. Compera D, Entchev E, Haritoglou C, et al. Lamellar hole-associated epiretinal proliferation in comparison to epiretinal membranes of macular pseudoholes. *Am J Ophthalmol*. 2015;160:373–384.
12. Bone RA, Landrum JT, Hime GW, et al. Stereochemistry of the human macular carotenoids. *Invest Ophthalmol Vis Sci*. 1993;34:2033–2040.
13. Snodderly DM, Brown PK, Delori FC, Auran JD. The macular pigment. I Absorbance spectra, localization, and discrimination from other yellow pigments in primate retinas. *Invest Ophthalmol Vis Sci*. 1984;25:660–673.
14. Snodderly DM, Auran JD, Delori FC. The macular pigment. II Spatial distribution in primates retinas. *Invest Ophthalmol Vis Sci*. 1984;25:674–685.
15. Bhosle P, Larson AJ, Frederick JM, et al. Identification and characterization of a Pi isoform of glutathione S-transferase (GSTP1) as a zeaxanthin-binding protein in the macular of the human eye. *J Biol Chem*. 2004;279:49447–49454.
16. Li B, Vachali P, Frederick JM, Bernstein PS. Identification of StARD3 as a lutein-binding protein in the macula of the primate retina. *Biochem*. 2011;50:2541–2549.
17. Dennison JL, Stack J, Beatty S, Nolan JM. Concordance of macular pigment measurements obtained using customized heterochromatic flicker photometry, dual-wavelength autofluorescence, and single-wavelength reflectance. *Exp Eye Res*. 2013;116:190–198.
18. Akuffo KO, Nolan JM, Stack J, et al. The impact of cataract, and its surgical removal, on measures of macular pigment using the Heidelberg Spectralis HRA+OCT multicolor device. *Invest Ophthalmol Vis Sci*. 2016;57:2552–2563.
19. Gellermann W, Ermakov IV, Ermakov MR, et al. In vivo resonant Raman measurement of macular carotenoid pigments in the young and the aging human retina. *J Opt Soc Am A*. 2002;19:1172–1186.
20. Gass JDM. Müller cell cone, an overlooked part of the anatomy of the fovea centralis. *Arch Ophthalmol*. 1999;117:821–823.
21. Yamada E. Some structural features of the fovea centralis in the human retina. *Arch Ophthalmol*. 1969;82:151–159.

Investigative Ophthalmology & Visual Science